Processing and Application of Ceramics 19 [4] (2025) 359–366
https://doi.org/10.2298/PAC2504359K

First-principles investigation of structure, electronic and optical properties of newly synthesized double perovskite Nd_2FeTiO_6 for optoelectronic applications

Mrityunjay Kumar[1,2], Rahul K. Singh[1], Sanat K. Mukherjee[3], Sumit K. Roy[4,*]

[1]*University Department of Physics, Ranchi University, Ranchi-834009, India*
[2]*School of Studies in Physics, Shaheed Mahendra Karma Vishwavidyalaya, Jagdalpur-494001, India*
[3]*Department of Physics, Birla Institute of Technology, Mesra, Ranchi 835215, Jharkhand, India*
[4]*Department of Physics, St. Xavier's College, Ranchi University, Ranchi-834001, India*

Received 22 September 2025; Received in revised form 25 November 2025; Accepted 4 December 2025

Abstract

Double perovskite Nd_2FeTiO_6 (NFTO) compound was comprehensively studied to evaluate its promising characteristics for optoelectronic applications. Structure, electronic and optical properties were analysed by first-principles calculations. The crystal structure of NFTO was found to be monoclinic with space group $P2_1/c$, and its structural stability was confirmed through calculated formation energy and octahedral factor, and also by experimental results. The electronic band structure analysis indicates an indirect bandgap of 0.57 eV using PBE-GGA and 1.513 eV with mBJ potential, aligning closely with the experimental value of 1.77 eV obtained from UV-visible spectroscopy. Detailed optical property investigations demonstrate significant absorbance in the UV-visible range, indicating multiple electronic transitions. Additionally, the dielectric function analysis of the compounds highlights promising dielectric properties and efficient light absorption, making NFTO a suitable candidate for solar cells, photovoltaic and other optoelectronic devices.

Keywords: *double perovskite, density functional theory, band gap, optical properties, dielectric function*

I. Introduction

The discovery of novel energy sources that are independent of fossil fuels is becoming increasingly important in view of the recent substantial growth in energy demand. As a result, renewable energy sources are receiving increasing global attention. Lead-free double perovskite compounds are recognized as an important class of materials in contemporary materials research and industry, because of their significant properties, including chemical flexibility and an extensive range of compositional forms [1–5]. Ordinary perovskite structure ABO_3, which has a wide variety of characteristics from insulators to superconductors, can be used to deduce the crystal structure of double perovskite. Since the two standard perovskite structures, ABO_3 and $AB'O_3$, make up the double perovskite compounds, the general chemical formula for double perovskites is $A_2BB'O_6$ with two dissimilar transition metal ions at the B and B' sites and an alkaline-earth or rare-earth metal ion at the A site. Researchers have recently discovered numerous double perovskites that could be utilized in solar cells, photovoltaic devices, photocatalysis and the storage of photochemical energy. The unique physical characteristics of double perovskite ($A_2BB'O_6$) compounds are significantly influenced by the arrangement of the BO_6 and $B'O_6$ octahedra.

Shah *et al.* [4] used GGA+U in the DFT framework to investigate the structural, electrical and optical characteristics of perovskites La_2MTiO_6 (M = Co, Ni, Cu and Zn). It was found that the compounds have a monoclinic structure and exhibit electronic band profiles similar to those of semiconductors with a band gap in the range of 1.02 to 2.3 eV. The analysed optical data of the compounds suggest that they can be used in optoelectronic devices. Boudad *et al.* [6] synthesized new double perovskite oxides, $RBaFeTiO_6$ (R = La, Eu) and examined their structural, electrical, and optical charac-

*Corresponding author: +91 9835342618
e-mail: *sumit.sxc13@gmail.com*

teristics. Direct band gaps reported for $LaBaFeTiO_6$ and $EuBaFeTiO_6$ were 3.75 and 3.53 eV, respectively. Structural, electrical and magnetic characteristics of double perovskite Sr_2FeReO_6 were analysed by Zhang *et al.* [7] using first-principles calculations. The electrical and optical characteristics of Gd_2FeCrO_6 double perovskite were calculated using the first-principles by Das *et al.* [8]. They observed a fair agreement between the experimental band gap of ~2.0 eV and that calculated theoretically (direct optical band gap) of ~1.99 eV [9]. Employing first-principles calculations, Zhang *et al.* [10] have examined the structural, electronic and magnetic characteristics of double-perovskite Ho_2MnFeO_6. They reported that the compound's ground state is half metallic and half ferrimagnetic, with monoclinic symmetry in space group $P2_1/c$. Manzoor *et al.* [11] examined the optoelectronic, mechanical, structural and thermoelectric characteristics of Sr_2BTaO_6 (B = Sb, Bi) using first-principles calculations pertaining to solar cell applications. As per the calculated electronic structure using the mBJ potential, indirect band gaps of 0.97 and 2.066 eV were obtained for Sr_2BTaO_6 (B = Sb, Bi) double perovskites, respectively, indicating their potential suitability for photovoltaic applications.

Therefore, this study aims to provide a comprehensive first-principles investigation of the double perovskite Nd_2FeTiO_6 (NFTO), and to compare the obtained results with experimental data.

II. Computational details and results

In this study, first-principles calculations were carried out using density functional theory (DFT) as implemented in the WIEN2k code [12], which employs the full-potential linearized augmented plane wave (FP-LAPW) method [13]. The structural optimization and electronic property calculations were initially performed using the Perdew-Burke-Ernzerhof (PBE) exchange-correlation functional within the generalized gradient approximation (GGA). To address the well-known underestimation of bandgap values by GGA, the modified Becke-Johnson (mBJ) potential was employed for more accurate electronic structure predictions.

The plane wave cut-off condition was set using $R_{MT} \times K_{max} = 7.0$, where R_{MT} denotes the smallest muffin-tin radius and K_{max} is the maximum modulus of reciprocal lattice vectors. The charge density Fourier expansion cutoff was set to $G_{max} = 12$ a.u.$^{-1}$. Brillouin zone integration was performed using a $10 \times 10 \times 10$ Monkhorst-Pack k-point mesh, corresponding to 1000 k-points in the irreducible wedge. The total energy convergence threshold for the self-consistent field (SCF) cycle was set to 10^{-5} Ry.

To evaluate the optical properties, the complex dielectric function and related quantities such as the refractive index, absorption coefficient and reflectance were calculated based on the electronic structure. All simulations were aimed at understanding the structural stability, electronic nature and optical response of the Nd_2FeTiO_6 (NFTO) compound.

In addition, a polycrystalline Nd_2FeTiO_6 sample was synthesized by a solid-state reaction, where stoichiometric amounts of Nd_2O_3, FeO and TiO_2 were mixed in an agate mortar and calcined at 1200 °C and sintered at 1300 °C. The detailed synthesis procedure is provided in our previous paper [14]. Crystal structure was analysed by X-ray diffractometer by using CuKα radiation (λ = 1.5405 Å), whereas UV-visible absorption measurements were performed for the exploration of the optical properties of the prepared sample.

2.1. Structural analysis

Two dimensionless quantities, namely, tolerance factor (t) and octahedron factor (μ), are used to predict the stability and form of perovskite/double perovskite structures. The tolerance factor broadly measures the size compatibility of all three ions (A, B, and X) in the perovskite structure and predicts the overall stability and possible structural distortions; whereas the octahedron factor specifically focuses on the fit of the B-site cation within the octahedral site formed by the anions, influencing the stability and shape of the BX_6 octahedra. As both factors are crucial for understanding and predicting the behaviour of perovskite materials, these parameters have been calculated for the synthesized double perovskite NFTO and found to be 0.902 and 0.4875, respectively. The octahedral factor (μ) for the NFTO compound, defined as the ratio of the B-site cation (Ti) radius to that of the surrounding anion, falls within the ideal range of 0.414 to 0.732. This indicates that the titanium ion is appropriately sized to occupy the octahedral site without causing distortion or collapse of the octahedral framework, thereby ensuring the structural stability of the compound. The tolerance factor of the NFTO compound is found to be 0.902, suggesting that the compound possesses either a monoclinic or orthorhombic structure.

Figure 1 shows the crystal structure of the double perovskite Nd_2FeTiO_6 with space group $P2_1/c$ generated by first-principle computational methods. XRD analysis indicates a monoclinic atomic arrangement for the compound. Details regarding this can be found in one of our earlier papers [14]. The structural characteristics of

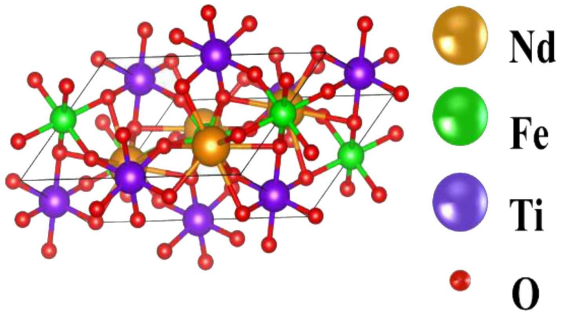

Figure 1. Generated crystal structure of Nd_2FeTiO_6 compound

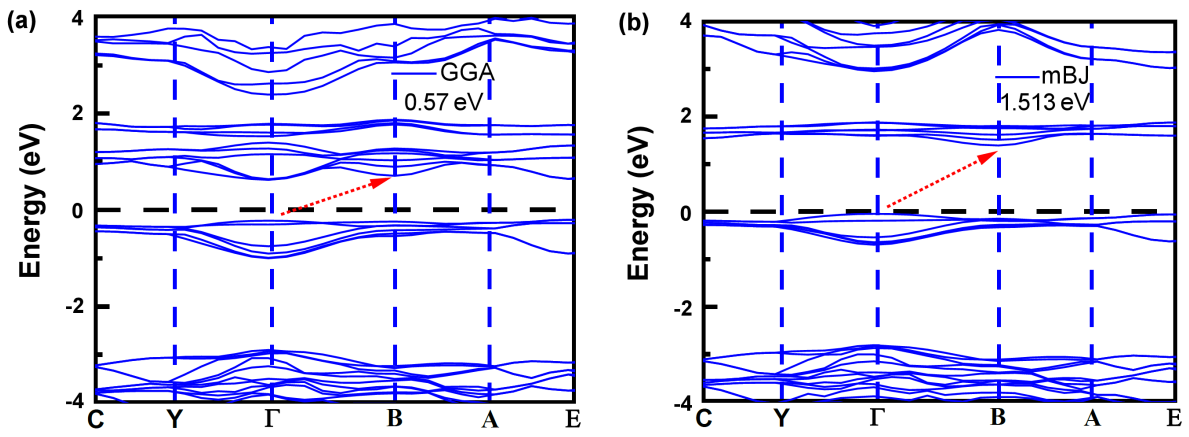

Figure 2. Band structure for monoclinic double perovskite Nd_2FeTiO_6 using: a) GGA and b) mBJ approximations

Table 1. Computed lattice parameters and their experimental values for the Nd_2FeTiO_6 compound [14]

Lattice parameter	Experimental value	Computed value
a [Å]	5.5218(7)	5.55674
b [Å]	5.4658(7)	5.38698
c [Å]	9.498(2)	9.3233
α [°]	90	90
β [°]	125.37(1)	124.96
γ [°]	90	90

the NFTO compound were optimized using the Perdew-Burke-Ernzerhof (PBE) function.

The computed and experimental values of lattice parameters are presented in Table 1.

2.2. *Electronic properties*

The charge density distribution technique was employed to study the electronic characteristics, such as the band structure, density of states (DOS) and bonding nature of double perovskite Nd_2FeTiO_6 (NFTO) [15].

Band structure

The electronic band structure of the NFTO double perovskite was computed along the high-symmetry directions (C–Y–Γ–B–A–E) in the Brillouin zone and presented in Figs. 2a and 2b. To improve the accuracy of the results, calculations were performed using multiple exchange-correlation functionals, including the Perdew-Burke-Ernzerhof generalized gradient approximation (PBE-GGA) and the modified Becke-Johnson (mBJ) potential. As the PBE-GGA approach is known to underestimate the band gap, the mBJ potential was employed to provide a more accurate estimation [16]. The indirect band gap of the NFTO compound was found to be 0.57 eV using PBE-GGA and 1.513 eV using the mBJ method.

Density of states (DOS)

The partial density of states (PDOS) and total density of states (TDOS) of NFTO, calculated using the modified Becke-Johnson (mBJ) potential, are shown in Fig. 3. The presence of a distinct band gap near the Fermi level confirms the semiconducting nature of the material, as also reflected by the more accurate band gap predicted using the mBJ method.

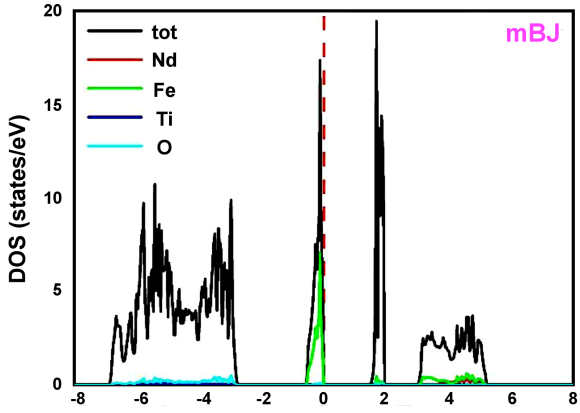

Figure 3. Calculated properties with TDOS electronic and PDOS for Nd_2FeTiO_6 compound

In the valence band region (from −8 eV to 0 eV), the total density of states (TDOS) exhibits multiple peaks, attributed to the hybridization of atomic orbitals from the constituent elements in NFTO. Analysis of the partial density of states (PDOS) shows that Nd *s*-states contribute minimally, indicating a limited role in bonding within this region. In contrast, Fe *d*-states dominate the upper portion of the valence band (around −1 eV to 0 eV), while O *p*-states are primarily located at lower energies (approximately −6 to −2 eV), signifying strong Fe–O and Ti–O orbital interactions. These hybridizations collectively shape the electronic structure and highlight the complex bonding environment in the NFTO.

In the conduction band, a sharp peak just above the Fermi level indicates that Fe *d*-states dominate the conduction band minimum, with only minor contributions from Ti *d*-states. These sharp features are typically associated with localized electronic states. The presence of a finite band gap, along with significant Fe *d*-state in-

volvement near the Fermi level, suggests that NFTO exhibits semiconducting behaviour with the potential for magnetic ordering [17]. These properties make NFTO a promising candidate for spintronic and multiferroic applications, where the interplay between electronic and magnetic interactions is essential.

Electron localization function (electron density)

The bonding characteristics of a material can be effectively analysed through its charge density and the spatial distribution of electrons [15]. This approach helps distinguish between different bonding types: covalent, metallic, and ionic. In covalent bonding, atoms share electrons, often resulting in a directional and sometimes asymmetric charge distribution, especially in the case of polar covalent bonds. Metallic bonding, on the other hand, features a 'sea' of delocalized electrons freely moving among positively charged metal ions, leading to a more diffuse charge distribution.

Ionic bonding is fundamentally different, involving a complete transfer of electrons from one atom to another, creating positively and negatively charged ions that interact via electrostatic forces. This typically results in localized charge densities around each ion with minimal overlap between the electron clouds.

In the case of NFTO, the calculated charge density plots (as shown in Fig. 4) reveal that the charge distributions around Nd, Fe and Ti atoms are nearly spherical, with no significant overlap between their charge contours and those of the surrounding O atoms. This spherical symmetry and lack of shared charge density suggest the formation of predominantly ionic bonds between oxygen and the metal cations [18]. The Bader charge analysis, summarized in Table 2, further supports this interpretation by quantifying the effective charge transfer between atoms, reinforcing the ionic character of bonding in the NFTO structure.

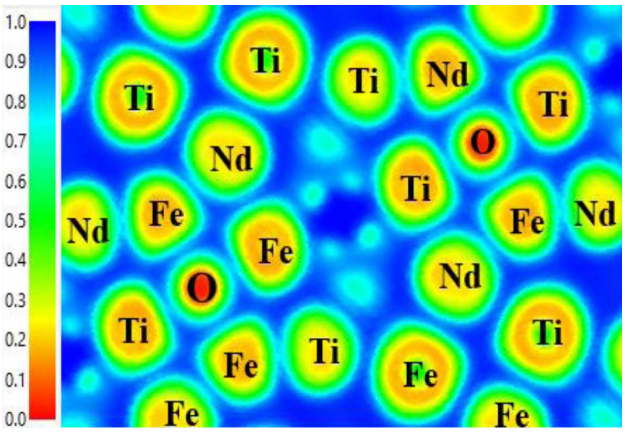

Figure 4. Electron localization function (ELF) for Nd_2FeTiO_6 compound along (100) plane

Table 2. Bader charge analysis for the Nd_2FeTiO_6 compound

Compound	GGA	nBJ	Bader charge
Nd_2FeTiO_6	0.57	1.513	Nd = 2.08 Fe = 2.07 Ti = 1.93 O = −1.24

2.3. Optical properties

UV-visible absorption spectra

UV-visible absorption measurements were performed for the exploration of the optical properties of the synthesized NFTO samples. From Fig. 5a, it is evident that NFTO exhibits multiple absorbance peaks (A1, A2, A3 and A4) in the UV and visible regions, representing a multiband electronic structure. The absorption peak around 373 nm is attributed to charge transfer transitions from the oxygen $2p$ orbital to the iron $3d$ orbital [O($2p$) → Fe($3d$)] within the FeO_6 octahedra [19,20]. The absorption peak near 600 nm is likely due to a p–p electronic transition [21]. Meanwhile, the peaks observed around 700 and 750 nm may be associated with d–d transitions within Fe^{2+} ions [21,22]. The optical bandgap of the prepared material was estimated using the Tauc equation:

$$(\alpha h\nu) = A(h\nu - E_g)^n \tag{1}$$

where α is the absorption coefficient, $h\nu$ represents the photon energy, A is a proportionality constant, E_g denotes the optical bandgap and n characterizes the nature of the electronic transition. Specifically, $n = 2$ corresponds to an allowed direct transition, while $n = 1/2$ indicates an allowed indirect transition [22,23]. As illustrated in Fig. 5b, the plot of $(\alpha h\nu)^{1/2}$ versus $h\nu$ yields a linear region and extrapolation of this linear portion to the photon energy axis reveals an indirect bandgap value of approximately 1.77 eV. This relatively narrow bandgap, in combination with the material's multiple absorption features in the UV-visible range, suggests that the synthesized NFTO material has promising optoelectronic properties [24,25].

Dielectric function and optical constants

The relatively moderate indirect bandgap of the double perovskite compound NFTO motivated this study, which focuses on investigating its optical properties, as their precise characterization is crucial for evaluating prospective application of NFTO in optoelectronic and photovoltaic applications [26]. In this context, the energy-dependent optical properties were evaluated through the complex dielectric function, which is expressed as:

$$\varepsilon(\omega) = \varepsilon_1(\omega) + i\varepsilon_2(\omega) \tag{2}$$

Here, $\varepsilon_1(\omega)$ represents the real part of the dielectric function, associated with the dispersion of the electromagnetic wave, while $\varepsilon_2(\omega)$ corresponds to the imaginary part, which accounts for transitions in intra-band and inter-band transitions from occupied to unoccupied states across the Brillouin zone (BZ) along k-vectors

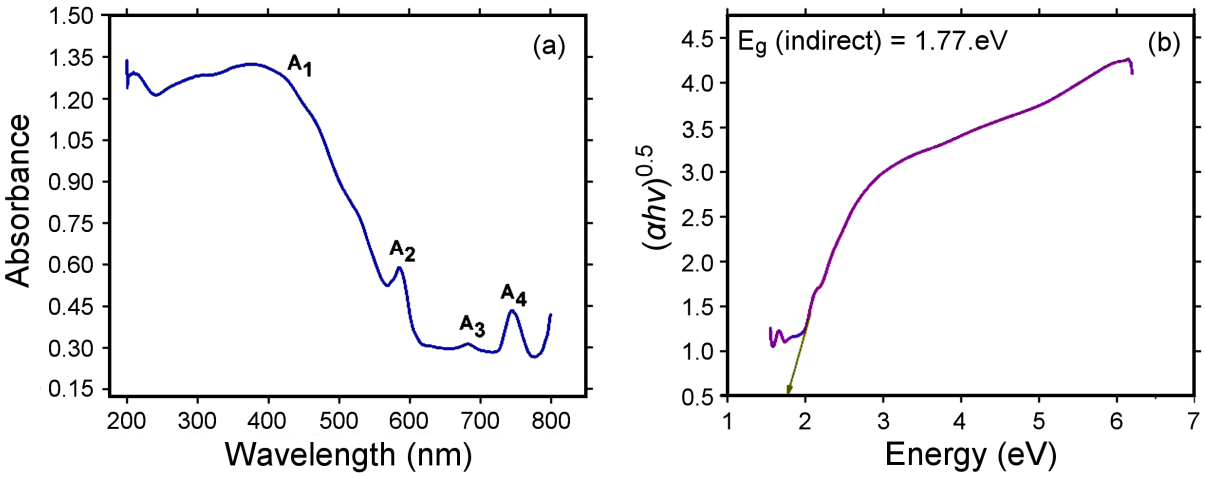

Figure 5. UV-visible absorption spectra of Nd_2FeTiO_6 compound (a) and corresponding Tauc plot (b)

[27,28]. By analysing these components, the optical behaviour of the material, such as refractive index, absorption coefficient and energy loss, can be thoroughly understood. This approach enables a comprehensive understanding of how the material interacts with incident electromagnetic radiation across different frequencies. The imaginary part $\varepsilon_2(\omega)$ can be mathematically expressed as:

$$\varepsilon_2(\omega) = \frac{e^2\hbar}{\pi m^2\omega^2}\sum\int |M_{v,c}(k)|^2\delta[\omega_{v,c}(k)-\omega]\mathrm{d}^3k \quad (3)$$

where ω is the photon angular frequency, e is the elementary charge (charge of the electron), $\hbar$ is reduced Planck's constant and $M_{v,c}(k)$ is the optical transition matrix element [29]. The $\varepsilon_1(\omega)$ can be computed using the Kramers-Kronig relation [29]:

$$\varepsilon_1(\omega) = 1 + \frac{2}{\pi}P\int_0^\infty \frac{\omega'\varepsilon_2(\omega')}{\omega'^2-\omega^2}\mathrm{d}\omega' \quad (4)$$

The variation of the real part $\varepsilon_1(\omega)$ and imaginary part $\varepsilon_2(\omega)$ components of the dielectric function for NFTO as a function of photon wavelength (ranging from 100 to 1500 nm) are presented in Fig. 6a. The real part of the dielectric function, $\varepsilon_1(\omega)$, represents the material's polarizability in response to an external electromagnetic field, essentially indicating how much the material becomes polarized when exposed to incident light [30]. The imaginary part, $\varepsilon_2(\omega)$, corresponds to the energy absorbed by the material due to electronic transitions, and it reflects optical losses associated with absorption processes. At higher wavelengths (i.e. lower photon energies), the value of $\varepsilon_1(\omega)$ approaches a constant, which is referred to as the static dielectric constant, denoted by $\varepsilon_1(0)$ [31,32]. This parameter is particularly important for understanding the low-energy optical and electronic behaviour of the material.

As shown in Fig. 6a, the real part of the dielectric function, $\varepsilon_1(\omega)$, increases with increasing photon energy (i.e. as the wavelength decreases) and exhibits several relaxation peaks. These peaks are indicative of polarization relaxation processes within the material and can be used to estimate the corresponding relaxation times or frequencies [32]. Additionally, the observed shift of the relaxation peaks toward lower photon ener-

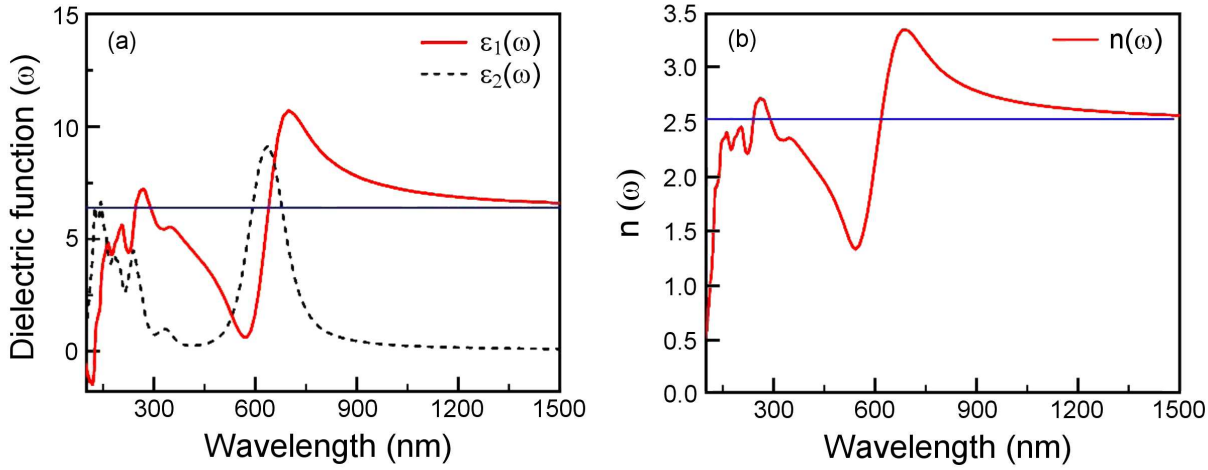

Figure 6. Computed: a) real (ε_1) and imaginary (ε_2) parts of dielectric function and b) refractive index, n

gies (i.e. longer wavelengths) suggests an inverse relationship between the relaxation frequency and the effective mass of the oscillating atoms or dipoles [33]. This behaviour is consistent with the dielectric relaxation theory, where heavier oscillating species lead to slower polarization response and thus lower relaxation frequencies. The principal peaks of the real part of the dielectric function, $\varepsilon_1(\omega)$, for the NFTO compound are located within the visible wavelength range, indicating significant polarization activity in this spectral region. Figure 6a also illustrates the variation of the imaginary part, $\varepsilon_2(\omega)$, with photon wavelength. Since $\varepsilon_2(\omega)$ is associated with optical absorption, it offers valuable insights into the material's absorption characteristics and optical bandgap [34,35]. No significant absorption is observed up to a photon energy of approximately 1.493 eV (corresponding to wavelengths between 1500 and 830 nm), suggesting that the material's optical bandgap closely matches its electronic (electrical) bandgap. The primary peak in $\varepsilon_2(\omega)$ near 600 nm (visible region) originates from O($2p$) $\rightarrow$ Fe($3d$) inter-band transitions, as supported by the PDOS (partial density of states) [36].

The refractive index $n(\omega)$ was calculated using the relation $n = \sqrt{\varepsilon_1}$. As shown in Fig. 6b, the refractive index exhibits a trend similar to that of $\varepsilon_1(\omega)$, reinforcing the relationship between the material's polarization and its optical response [11,37]. The static refractive index $n(0)$, representing the value at zero photon energy, is summarized in Table 3.

The reflectance spectrum $R(\omega)$, presented in Fig. 7a, provides insight into the surface optical response of NFTO. The reflectance increases from near-zero at low energies $R(0)$ to a maximum in the region with minimal absorption. With increasing photon energy, the reflectance rises and reaches a peak at approximately 630 nm. Variations in peak intensity are attributed to the differences in photon interactions at the material's surface, including interference effects and the angle of incidence [37].

Figure 7b demonstrates how the absorption coefficient changes with photon energy. The peak must represent the energy lost due to the material absorption because it exhibits the same pattern as $\varepsilon_2(\omega)$. The visible spectrum's absorption peaks demonstrate the compounds under investigation's strong absorption capabilities [38].

Table 3. Calculated value of optical constants for the Nd_2FeTiO_6 compound

Optical property	Computed value
$\varepsilon_1(0)$	6.55
$n(0)$	2.57
$R(0)$	0.2

III. Conclusions

In this study, the electronic, structural and optical properties of the double perovskite Nd_2FeTiO_6 (NFTO) were thoroughly studied. Structural analysis confirms that the material crystallizes in a monoclinic structure with space group $P2_1/c$. The electronic band structure calculations using both the PBE-GGA and the modified Becke-Johnson (mBJ) exchange potential reveal indirect bandgap values of 0.57 and 1.513 eV, respectively. The experimental optical bandgap, determined via UV-visible spectroscopy, was found to be approximately 1.77 eV. This value is in good agreement with the bandgap obtained through the mBJ functional, validating the reliability of the theoretical model.

To further understand the optical behaviour of NFTO, an extensive analysis of the energy-dependent optical functions was carried out. The dielectric function components $\varepsilon_1(\omega)$ and $\varepsilon_2(\omega)$ revealed strong polarization effects and absorption features within the visible range. The absence of absorption below 1.493 eV confirmed the wide bandgap nature of the material. Additional optical parameters, incorporating the refractive index $n(\omega)$ and reflectance $R(\omega)$, were also examined. The refractive index showed a strong correlation with $\varepsilon_1(\omega)$, and reflectance analysis indicated surface-dependent optical responses, with a peak observed near 630 nm.

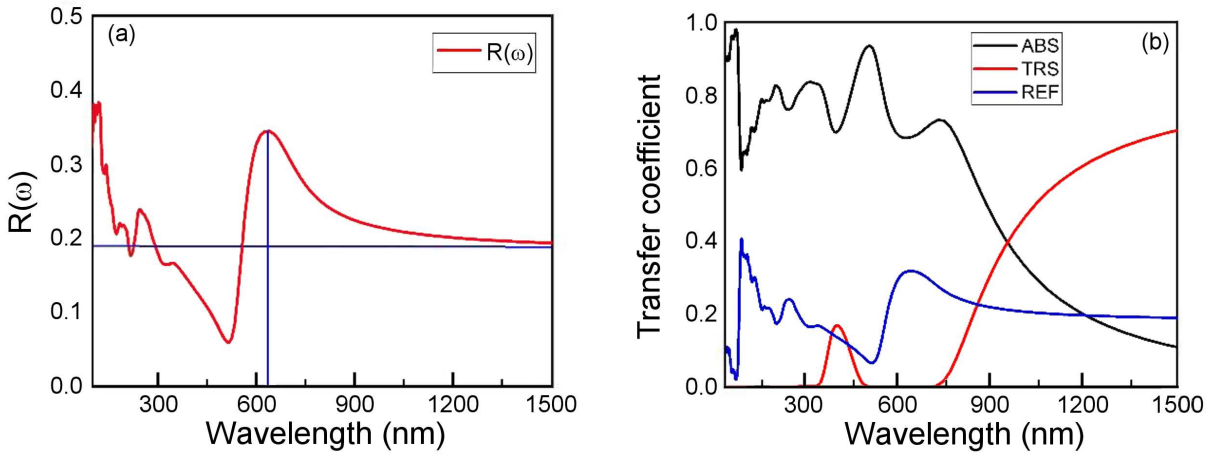

Figure 7. Computed: a) spectral reflectance $R(\omega)$ and b) transfer $T(\omega)$ and absorption $\alpha(\omega)$ coefficients for Nd_2FeTiO_6 compound

The results suggest that NFTO exhibits excellent dielectric behaviour and significant light absorption capabilities across a broad spectral range. These properties make NFTO a promising candidate for applications in optoelectronic and photovoltaic devices. The combination of theoretical and experimental insights contributes to a deeper understanding of the NFTO's potential in energy-related technologies.

Acknowledgement: One of the authors, Mrityunjay Kumar, would like to thank UGC, New Delhi, India, for providing the financial support (MAY18-524009).

References

1. S. Vasala, M. Karppinen, "$A_2B'B''O_6$ perovskites: A review", *Prog. Solid State Chem.*, **43** (2015) 1–36.
2. H. Das, UV. Waghmare, T. Saha-Dasgupta, D.D. Sarma, "Electronic structure, phonons, and dielectric anomaly in ferromagnetic insulating double pervoskite La_2NiMnO_6", *Phys. Rev. Lett.*, **100** (2008) 186402.
3. H.-R. Fuh, Y.-P. Liu, S.-H. Chen, Y.-K. Wang, "Electronic structures of compensated magnetism in double perovskites $A_2CrRu(Os)O_6$ (A = Si, Ge, Sn, and Pb) from ab initio calculations", *J. Alloys Compd.*, **547** (2013) 126–131.
4. S. Shah, Z. Ali, S. Mehmood, I. Khan, I. Ahmad, "Electronic structure, optical and magnetic properties of double perovskites La_2MTiO_6 (M = Co, Ni, Cu and Zn)", *Mater. Chem. Phys.*, **272** (2021) 125050.
5. Y.P. Liu, H.R. Fuh, Z.R. Xiao, Y.K. Wang, "Theoretical prediction of half-metallic materials in double perovskites $Sr_2Cr(Co)B'O_6$ (B' = Y, La, Zr, and Hf) and $Sr_2V(Fe)B'O_6$ (B' = Zr and Hf)", *J. Alloys Compd.*, **586** (2014) 289–294.
6. L. Boudad, M. Taibi, A. Belayachi, M. Abd-lefdil, "Structural, morphological, dielectric and optical properties of double perovskites $RBaFeTiO_6$ (R = La, Eu)", *RSC Adv.* **11** (2021) 40205–40215.
7. Z. Zhang, H. Yan, Z. Huang, X. Chi, C. Li, Z.S. Lim, S. Zeng, K. Han, G.J. Omar, K. Jin, A. Ariando, "Tunable magnetic properties in Sr_2FeReO_6 double-perovskite", *Nano Lett.*, **22** (2022) 9900–9906.
8. S. Das, M.D.I. Bhuyan, M.A. Basith, "First-principles calculation of the electronic and optical properties of Gd_2FeCrO_6 double perovskite: Effect of Hubbard U parameter", *J. Mater. Res. Technol.*, **13** (2021) 2408–2418.
9. N. Masta, D. Triyono, H. Laysandra, "Investigation of electrical conductivity and dielectric properties of Sr_2FeTiO_6", *IOP Conf. Ser. Mater. Sci. Eng.*, **496** (2019) 012010.
10. J.T. Zhang, X.M. Lu, J. Zhou, J. Su, K.L. Min, F.Z. Huang, J.S. Zhu, "First-principles study of structural, electronic, and magnetic properties of double perovskite Ho_2MnFeO_6", *Phys. Rev. B*, **82** (2010) 224413.
11. M. Manzoor, D. Bahera, R. Sharma, F. Tufail, M.W. Iqbal, S.K. Mukherjee, "Investigated the structural, optoelectronic, mechanical, and thermoelectric properties of Sr_2BTaO_6 (B = Sb, Bi) for solar cell applications", *Int. J. Energy Res.*, **46** (2022) 23698–23714.
12. P. Blaha, K. Schwarz, F. Tran, R. Laskowski, G.K.H. Madsen, L.D. Marks, "WIEN2k: An APW+lo program for calculating the properties of solids", *J. Chem. Phys.*, **152** (2020) 074101.
13. S. Nazir, N.A. Noor, M. Manzoor, A. Dahshan, "Ab-initio simulations of Li-based double perovksites $A_2LiInBr_6$ (A = Rb, Cs) for solar cell applications", *Chem. Phys. Lett.*, **798** (2022) 139612.
14. M. Kumar, S. Roy, R. Singh, K. Prasad, "Double perovskite Nd_2FeTiO_6 ceramics: Structural and electrical properties", *Process. Appl. Ceram.*, **17** (2023) 428–435.
15. D. Behera, R. Sharma, H. Ullah, H.S. Waheed, S.K. Mukherjee, "Electronic, optical, and thermoelectric investigations of Zintl phase AAg_2Se_2 (A=Sr, Ba) compounds: A first-principle approach", *J. Solid State Chem.*, **312** (2022) 123259.
16. D. Behera, S.K. Mukherjee, "Theoretical investigation of the lead-free K_2InBiX_6 (X = Cl, Br) double perovskite compounds using Ab initio calculation", *JETP Lett.*, **116** (2022) 537–546.
17. D.P. Rai, A. Shankar, M.P. Ghimire, Sandeep, R.K. Thapa, "The electronic, magnetic and optical properties of double perovskite A_2FeReO_6 (A = Sr, Ba) from first principles approach", *Comput. Mater. Sci.*, **101** (2015) 313–320.
18. M. Manzoor, D. Behera, R. Sharma, A.J.A. Moayad, A.A. Al-Kahtani, Y.A. Kumar, "Comprehensive first principles to investigate optoelectronic and transport phenomenon of lead-free double perovskites Ba_2AsBO_6 (B = Nb, Ta) compounds", *Heliyon*, **10** (2024) e30109.
19. M. Dhilip, S. Rameshkumar, R.K. Raji, T. Ramachandran, J.S. Punitha, F.R.M. Sundar Raj, K. Saravana Kumar, V. Anbarasu, N. Sekar, R. Chinnathambi, A.A. Ghfar, "Combined experimental and theoretical investigation on the structural, electronic, magnetic and optical properties of Pr_2CoFeO_6 double perovskite", *Mater. Today Commun.*, **38** (2024) 108120.
20. T. Arima, Y. Tokura, J.B. Torrance, "Variation of optical gaps in perovskite-type 3*d* transition-metal oxides", *Phys. Rev. B*, **48** (1993) 17006–17009.
21. M.D.I. Bhuyan, S. Das, M.A. Basith, "Sol-gel synthesized double perovskite Gd_2FeCrO_6 nanoparticles: Structural, magnetic and optical propertie", *J. Alloys Compd.*, **878** (2021) 160389.
22. V.M. Gaikwad, M. Brahma, R. Borah, S. Ravi, "Structural, optical and magnetic properties of Pr_2FeCrO_6 nanoparticles", *J. Solid State Chem.*, **278** (2019) 120903.
23. S. Bhattacharjee, B. Mohanty, N.C. Nayak, R.K. Parida, B.N. Parida, "Optical, dielectric and magnetic investigation of vanadium based double perovskite", *Mater. Sci. Semicond. Process.*, **123** (2021) 105503.
24. K. Yi, Q. Tang, Z. Wu, X. Zhu, "Unraveling the structural, dielectric, magnetic, and optical characteristics of nanostructured La_2NiMnO_6 double perovskites", *Nanomaterials*, **12** (2022) 979.
25. S. Mishra, R.N.P. Choudhary, S.K. Parida, "Structural, dielectric, electrical and optical properties of a double perovskite: $BaNaFeWO_6$ for some device applications", *J. Mol. Struct.*, **1265** (2022) 133353.
26. S. Wu, Z. Chen, H.-L. Yip, A.K.-Y. Jen, "The evolution and future of metal halide perovskite-based optoelectronic devices", *Matter*, **4** (2021) 3814–3834.
27. M. Gajdoš, K. Hummer, G. Kresse, J. Furthmüller, F. Bechstedt, "Linear optical properties in the projector-augmented wave methodology", *Phys. Rev. B*, **73** (2006) 045112.
28. D. Bensaid, B. Doumi, S. Ahmad, "Lithium doping effect for enhancing thermoelectric and optoelectronic per-

formance of Co_2NbAl", *JETP Lett*., **115** (2022) 539–547.
29. J.A. Abraham, G. Pagare, S.P. Sanyal, "Electronic structure, electronic charge density, and optical properties analysis of GdX_3 (X = In, Sn, Tl, and Pb) compounds: DFT calculations", *Indian J. Mater. Sci.*, **2015** [1] (2015) 296095.
30. D.R. Penn, "Wave-number-dependent dielectric function of semiconductors", *Phys. Rev*., **128** (1962) 2093–2097.
31. A. Ayyaz, Q. Mahmood, G. Murtaza, A.A. Abd El-Moula, S. Al-Qaisi, N. Sfina, A.S. Alshomrany, "Study of mechanical, optoelectronic, and thermoelectric properties of Rb_2ScAuZ_6 (Z = Br, I) for energy harvesting applications", *Inorg. Chem. Commun*., **165** (2024) 112520.
32. S.A. Khattak, S.M. Wabaidur, M.A. Islam, M. Husain, I. Ullah, S. Zulfiqar, G. Rooh, N. Rahman, M.S. Khan, G. Khan, T. Khan, B. Ghlamallah, "First-principles structural, elastic and optoelectronics study of sodium niobate and tantalate perovskites", *Sci. Rep*., **12** (2022) 21700.
33. M. Faizan, K.C. Bhamu, G. Murtaza, X. He, N. Kulhari, M.M. AL-Anazy, S.H. Khan, "Electronic and optical properties of vacancy ordered double perovskites A_2BX_6 (A = Rb, Cs; B = Sn, Pd, Pt; and X = Cl, Br, I): A first principles study", *Sci. Rep*., **11** (2021) 6965.
34. D. Behera, M. Manzoor, M.W. Iqbal, S. Lakra, S.K. Mukherjee, "Revealing excellent electronic, optical, and thermoelectric behavior of Eu based $EuAg_2Y_2$ (Y = S/Se): For solar cell applications", *Comput. Condensed Matter*, **32** (2022) e00723.
35. D. Behera, S.K. Mukherjee, "Optoelectronics and transport phenomena in Rb_2InBiX_6 (X = Cl, Br) compounds for renewable energy applications: A DFT insight", *Chemistry*, **4** (2022) 1044–1059.
36. K. Bouferrache, M.A. Habila, M.A. Ghebouli, S. Alomairy, F.K. Alanazi, M. Fatmi, B. Ghebouli, "Ferromagnetic and half metallic properties of $BaFeO_3$ and $CaFeO_3$ for spintronic applications", *Sci. Rep.*, **15** [1] (2025) 37093.
37. R.L.Z. Hoye, L. Eyre, F. Wei, F. Brivio, A. Sadhanala, S. Sun, W. Li, K.H.L. Zhang, J.L. MacManus-Driscoll, P.D. Bristowe, R.H. Friend, A.K. Cheetham, F. Deschler, "Fundamental carrier lifetime exceeding 1 μs in $Cs_2AgBiBr_6$ double perovskite", *Adv. Mater. Interfaces*, **5** [15] (2018) 180464.
38. M. Houari, B. Bouadjemi, A. Abbad, T. Lantri, S. Haid, W. Benstaali, M. Matougui, S. Bentata, "Lead-free semiconductors with high absorption: Insight into the optical properties of $K_2GeSnBr_6$ and K_2GeSnI_6 halide double perovskites", *JETP Lett*., **112** (2020) 364–369.